

## Cr/Al Oxide as Solid Acid Catalyst to Afford Babassu Biodiesel

Carla V. R. Moura,<sup>\*,a</sup> Haroldo L. S. Neres,<sup>a</sup> Mariane G. Lima,<sup>a</sup> Edmilson M. Moura,<sup>a</sup>  
Jose M. Moita Neto,<sup>a</sup> José E. de Oliveira,<sup>b</sup> José R. O. Lima,<sup>c</sup> Ilza M. Sttolin<sup>d</sup> and  
Eugênio C. E. Araújo<sup>d</sup>

<sup>a</sup>Departamento de Química, Universidade Federal do Piauí-UFPI, 64049-550 Teresina-PI, Brazil

<sup>b</sup>Centro de Monitoramento e Pesquisa em Qualidade de Combustíveis, Biocombustíveis,  
Petróleo e Derivados, CEMPEQC-DQO, Instituto de Química, Universidade Estadual Paulista -  
UNESP, 14800-060 Araraquara-SP, Brazil

<sup>c</sup>Centro de Ciências Exatas e Tecnológicas, Universidade Federal do Maranhão,  
65080-805 São Luis-MA, Brazil

<sup>d</sup>Embrapa Meio Norte, 64006-245 Teresina-PI, Brazil

In this work, it was described the preparation and the characterization of a solid acid catalyst obtained by the mixture of Cr/Al oxides (CRAL). The catalyst was tested in the transesterification reaction of babassu oil with 5% of free fatty acid (FFA). The results of textural and acidity characteristics of CRAL were: area ( $56 \text{ m}^2 \text{ g}^{-1}$ ), pore size ( $7.0 \text{ }\mu\text{m}$ ), total acidity ( $182.28 \text{ }\mu\text{mol g}^{-1}$ ), wherein Brønsted sites are the most active. Powder X-ray diffractometry (XRD), scanning electron microscopy (SEM) and energy-dispersive X-ray spectroscopy (EDX) show three phases of the catalyst ( $\text{Cr}_2\text{O}_3/\text{Na}_2\text{Cr}_2\text{O}_7/\text{Al}_2\text{O}_3$ ), 0.25:0.25:0.50, respectively. The reaction reached conversion about 98.6% under the conditions: alcohol/oil molar ratio (24:1), catalyst to oil mass ratio of 3.0%, 15 h and 70 °C. The turnover frequency (TOF) found was  $24.5 \times 10^{-4} \text{ s}^{-1}$ . Kinetic of the reaction was researched over a temperature range of 60-80 °C. A pseudo first-order model was proposed with the activation energy ( $E_a$ ) of  $49.18 \text{ kJ mol}^{-1}$ . CRAL is active in the biodiesel production for just one cycle, because in the second one it loses its activity. The leaching of catalyst is about 13%, demonstrating that the catalyst is not totally heterogeneous.

**Keywords:** biodiesel, catalyst, babassu oil, kinetic, reusability, leaching, heterogeneity

### Introduction

The development of new solids catalysts for use in chemical reactions has become in recent years a major technological challenge for the industries and research institutions, mainly in petrochemicals industries.<sup>1</sup> A process of obtaining cheaper and more efficient biodiesel has become one line of research, involving catalysts for obtaining biofuels. The main industrial process to obtain biodiesel is the transesterification or alcoholysis of vegetable oils with short chain alcohol using homogeneous catalysis, being most used basic catalysts, such as hydroxides, carbonates, sodium, and potassium alkoxides.<sup>2</sup> However, alkali catalysts are very sensitive to water and free fatty acid (FFA) content in virgin oils. The FFA present in oil can react with the alkaline catalyst to form

undesired byproducts, like soap and emulsion, and hinder the purification process of the product (biodiesel).<sup>3</sup>

For the purpose of producing biodiesel using alkali catalyst, the oil should go through purification processes such as neutralization and degumming. These processes increase the price of oil, which in turn increases the price of biodiesel. To reduce production costs of biodiesel, ideally, low quality oils or virgin oils are used. Notwithstanding, these oils contain a large amount of water and FFA, which prevents the use of alkali catalysts as mentioned. The homogeneous acid catalysts, like sulfuric acid, hydrochloric acid and sulfonic acid are also widely used,<sup>4</sup> and they show less sensitivity to FFAs and are able to conduct esterification and transesterification simultaneously.<sup>5,6</sup>

Meanwhile, the homogeneous acid catalyst is not preferred in the biodiesel production due to their lower activities compared with conventional alkaline catalysts. When the homogeneous acid catalysts are used in a higher

\*e-mail: carla@ufpi.edu.br

reaction temperature, a higher molar ratio of methanol to oil, and a longer reaction time are required.<sup>7,8</sup> Development of efficient, low cost and environmentally benign heterogeneous catalysts for transesterification of vegetable oils can lead to a much lower total production cost of biodiesel. Heterogeneous catalysts can be basic, acidic or biological (enzymatic) types. Solid acids favor both esterification and transesterification reactions simultaneously for biodiesel with high FFA.<sup>9</sup> Because of that, the focus of recent advances is in the rational development of recyclable solid acid catalyst. Solid acid catalysts (Lewis or Brønsted) are advantageous when compared to heterogeneous base catalysts and mineral acids.<sup>10</sup> Commercialization of inorganic heterogeneous catalysts for biodiesel production is still in the early stage. The development of new and cost effective heterogeneous acid catalysts can simplify significantly the manufacturing process and it can use low-cost feedstock and then reduce the final cost of biodiesel.<sup>3</sup>

The heterogeneous catalysts have some drawback, for example, in their preparation, reaction conditions, and leaching. All this drawbacks can increase production costs. Furthermore, for a catalyst to be considered heterogeneous, it should not leach, should be able to be reused, have high selectivity for the desired product and provide high yield and conversion.<sup>11</sup>

Many solid acid catalysts are described in the literature for the preparation of biodiesel (in many cases using oils with high FFAs content) such as sulfated zirconia,<sup>12</sup> tungstated zirconia (WZ),<sup>13</sup> ZnO-TiO<sub>2</sub>/Al<sub>2</sub>O<sub>3</sub>,<sup>14</sup> Fe<sup>3+</sup>-vanadyl phosphate,<sup>15</sup> SiO<sub>2</sub>-*N*-propyl sulfamic acid,<sup>16</sup> Zn/I<sub>2</sub>.<sup>17</sup> Aluminium phosphate and aluminium oxide are used as a support for a variety of acid catalysts. For example, Co/AlPO<sub>4</sub>, Fischer Tropsch process,<sup>18</sup> WO<sub>3</sub>/AlPO<sub>4</sub> transesterification reactions of soybean,<sup>19</sup> CeO<sub>2</sub>/ZrO<sub>2</sub>/Al<sub>2</sub>O<sub>3</sub> ternary oxides preparations,<sup>20</sup> Cu/SiO<sub>2</sub>/Al<sub>2</sub>O<sub>3</sub> 3-methylindole,<sup>21</sup> ZrO<sub>2</sub>/Al<sub>2</sub>O<sub>3</sub> propionitrile synthesis.<sup>22</sup> In this work, it was described the use of Cr<sub>2</sub>O<sub>3</sub>/Na<sub>2</sub>Cr<sub>2</sub>O<sub>7</sub>/Al<sub>2</sub>O<sub>3</sub> as an acid catalyst for the transesterification reaction of virgin babassu oil with methanol. The catalytic performance in the transesterification reaction was investigated regarding the conversion to methyl ester. The experimental variables such as the amount of catalyst, oil/methanol molar ratio and reaction time were investigated to optimize the transesterification conditions. The kinetic study (order and turnover frequency-TOF), reusability, solubility and heterogeneity tests of catalyst were investigated. Moreover, the catalyst was characterized by various techniques such as powder X-ray diffractometry (XRD), thermogravimetry (TG), scanning electron microscopy (SEM), infrared (FTIR), Brunauer-Emmett-Teller (BET) and energy-dispersive X-ray spectroscopy (EDX).

## Experimental

### Babassu oil

Crude babassu oil was donated by EMBRAPA Meio Norte (Brazilian Company of Agriculture and Livestock). The babassu oil used in this work had average molar mass of 879.71 g mol<sup>-1</sup>, with fatty acid distribution: octanoic acid (3.92%), decanoic acid (4.26%), dodecanoic acid (38.92%), tetradecanoic acid (14.50%), hexadecanoic acid (9.52%), octadecanoic acid (0.85%), (9Z)-octadec-9-enoic acid (14.92%), (9Z,12Z)-9,12-octadecadienoic acid (12.15%), (9Z,12Z,15Z)-9,12,15-octadecatrienoic acid (0.95%). The oil was washed with heated water, filtered, heated at 100 °C and then dried with CaSO<sub>4</sub>, achieving 5.0% of acidity. Chromium nitrate, aluminum nitrate, methyl alcohol and the standard substances for gas chromatography (GC) analysis were all purchased from Aldrich and Synth.

### Instrumentation

FTIR spectra were acquired in a spectrophotometer Bomen, Series MB, with 4 cm<sup>-1</sup> resolution and 32 cumulative scans. The samples were diluted in KBr containing 1 wt.%, and pressed to get tablet form. The X-ray diffractograms were obtained in a Rigaku-Rotaflex diffractometer with rotating anode, using monochromatic CuK $\alpha$  radiation ( $\lambda = 1.54056 \text{ \AA}$ ) and graphite monochromator. The voltage of the tube emission of copper was 40 kV and the filament current was 150 mA with a variation of  $2\theta$  from 5° to 75°. The diffractograms obtained were compared with the JCPDS-ICDD cards (Joint Committee on Powder Diffraction Standards-International Center for Diffraction Data) available in the Crystallographic Search Match software. The specific surface area was determined by Brunauer-Emmett-Teller multipoint through adsorption and desorption of nitrogen obtained by the Autosorb 1-Quantachrome Instruments equipment. The thermogravimetric curves were obtained in a TGA-2050 thermal analyzer from TA Instruments. It was used aluminium pot with a hole in the cap of approximately 0.5 mm in diameter and about 10 mg of the sample. The conditions of analysis were: sample thermal equilibrium at 30 °C, followed by heating rate of 10 °C *per* minute to 900 °C for catalysts and 600 °C for biodiesels, using nitrogen gas flow of 50 mL min<sup>-1</sup>. The loss of mass of the sample was determined as the difference between the initial and final mass. Data treatments were done with Origin software 8.0. The catalyst (CRAL) was analyzed in a Topcon SM-300 microscope, where the sample was fixed in carbon tape double sided with plating gold for 1 minute, using a current of 20 mA and beam acceleration of 15 kV;

increases ranged 150-3000 times. EDX was performed in a Shimadzu fluorescence X-ray spectrometer, EDX-800, in which the samples were placed in a container suitable for analysis. The generator of X-ray tube with rhodium (Rh) was operated in a voltage of 50 kV and 20 mA. The fatty acid methyl ester (FAME) content was determined using gas chromatograph (GC), where the analyzes were prepared by adding exactly 50 mg of the BIOCRAL, 0.2 mL of methyl heptadecanoate solution in heptane ( $5.082 \text{ mg mL}^{-1}$ ) as the internal standard. The equipment used to analyze the FAME was a Shimadzu, QP 2010 GC-FID model, equipped with a capillary column (DB-5HT, 0.32 mm, 30 m, 0.1  $\mu\text{m}$  film thickness). Samples were injected at an oven temperature of 70 °C. After an isothermal period of 1 min, the GC oven was heated at 15 °C  $\text{min}^{-1}$  to 190 °C, at 7 °C  $\text{min}^{-1}$  to 260 °C and at 20 °C  $\text{min}^{-1}$  to 380 °C, held for 10 minutes. Nitrogen was used as carrier gas. The temperature of the injector and detector were both set at 380 °C. The sample injection volume was of 1  $\mu\text{L}$  and the peak identification was made through comparing the retention times between the sample and the standard substances. The physicochemical properties of biodiesels were obtained according to official methods accepted by the National Agency of Petroleum, Natural Gas and Biofuels (ANP), ASTM 445, ASTM D 4052, ASTM-6304, EN-14104, EN-14111, EN-14110, ASTM D 4294, ASTM D130, ASTM D-6371, EN-3679. Levels of free and total glycerin, mono-, di-, and triglycerides were measured using a Shimadzu gas chromatograph, GC-FID QP 2010 model, in accordance with the described by ASTM D-6584.

## Synthesis

### Catalyst

25 mL of a chromium nitrate solution ( $1.25 \text{ mol L}^{-1}$ ), and 62.5 mL of aluminium nitrate solution ( $1.25 \text{ mol L}^{-1}$ ) were mixed and heated to 60 °C. Then, sodium carbonate solution ( $1.25 \text{ mol L}^{-1}$ ) was slowly added (dropwise) until forming a precipitate and the system acquiring pH of 8.5. After the precipitation, the system was stirred and heated (60 °C) for 2 h. Then, the mixture was centrifuged and the precipitate was washed with distilled water. The solid was dried at room temperature and calcined at 500 °C for 12 hours. This catalyst was called CRAL.

### Biodiesel

Transesterification reactions were carried out in a 250 mL three-necked glass reactor equipped with a water-cooled condenser, a magnetic stirrer and a thermometer with different volumes of methanol and varied amounts of catalyst. First, the catalyst and alcohol

were stirred for 30 min, and then, 40 g of babassu oil was added at the reactor, and heated at 70 °C. The catalyst and glycerol were separated from the mixture by centrifugation at 15,000 rpm for 2 minutes, and the biodiesel was washed with water to remove some undesirable product or reagent. After that, the biodiesel was dried with  $\text{Na}_2\text{SO}_4$ .

### Acidity of catalyst

The acidity of the catalyst was calculated using pyridine technique coupled to FTIR. The catalyst was dried in a nitrogen atmosphere and heated to 450 °C *in vacuo* to remove the adsorbed material. Subsequently, steam of  $\text{N}_2$  was passed through a wash bottle containing pyridine, and steam of pyridine/ $\text{N}_2$  was passed through the catalyst for 2 hours. The IR spectra were measured when the sample was at 150 °C, 250 °C and 350 °C.

Calculation of concentration of Lewis and Brönsted acidic sites was derived from Emeis,<sup>23</sup> (equation 1), where IMEC is the integrated molar extinction coefficient,  $\epsilon$  = molar extinction coefficient ( $\text{dm}^3 \text{ mol}^{-1} \text{ cm}^{-1}$ ) and  $\sigma$  = wavenumber ( $\text{cm}^{-1}$ ).

$$\text{IMEC} = \int \epsilon \cdot d\sigma \quad (1)$$

Emeis<sup>23</sup> showed that the integrated molar extinction coefficient (IMEC) varied only in relation to the wavelength ( $\sigma$ ), and it differs for the adsorption of Brönsted band [IMEC (B)] and Lewis band [IMEC (L)]. The values are  $1.67 \text{ cm } \mu\text{mol}^{-1}$  and  $2.22 \text{ cm } \mu\text{mol}^{-1}$  to Brönsted and Lewis bands, respectively. These values allowed reaching equations 2 and 3, which are responsible for the calculation of pyridine adsorbed on the acid sites and, therefore, the concentration of Brönsted and Lewis sites, considering the site stoichiometric acid/pyridine factor equal to unity.

$$C(\text{B}) = 1.88 \times \text{IA}(\text{B}) \times R^2/W \quad (2)$$

$$C(\text{L}) = 1.42 \times \text{IA}(\text{B}) \times R^2/W \quad (3)$$

$C(\text{B})$  and  $C(\text{L})$  are concentration of acidic sites of Brönsted and Lewis ( $\mu\text{mol g}^{-1}$ ), IA is the integrated absorbance of B or L band ( $\text{cm}^{-1}$ ), R is the radius of catalyst disk (cm) and W is the weight of disk (mg). The radius and weight of disk used to measure absorption in IR were: 0.001 cm and 10 mg, respectively.

### Turnover frequency (TOF)

The turnover frequency (TOF) was calculated by using equation 4.<sup>24</sup> The calculations are available in the Supplementary Information (SI) section.

TOF = [Amount of products/amount of active sites × time] (4)

### Reusability of the catalyst

The reusability of the catalyst was tested to check its capacity to provide sustainable catalytic activity, and the leaching test was accomplished to estimate the homogeneous contribution of catalyst at reaction. The experimental runs were conducted at methanol/oil molar ratio of 24:1, catalyst to oil mass ratio of 3.0%, reaction time of 15 h. After the reaction, the catalyst was separated by filtration and washed with petroleum ether and methanol to remove glycerin and undesired material attached on its surface. It was dried at 120 °C for 24 h, and calcined at 500 °C for 12 h, before reused in the subsequent runs.

### Leaching and heterogeneity test

Besides, the leaching of the active component of the catalyst was tested by placing the catalyst in contact with methanol for 8 h at 70 °C. The catalyst was separated by filtration, and the filtrate was allowed to react up with oil for 8 h to complete de reaction time (15 h), in the same conditions. The procedure contacting the methanol and the catalyst was repeated until the fourth time using the catalyst recovered from previous runs. The conversion into ester was measured by GC.

## Results and Discussion

### Catalyst characterization

Infrared spectra (Figure S1) of the CRAL showed a broadband between 3550-3225  $\text{cm}^{-1}$ , which was attributed to the stretching of the O–H bond, and a band at 1630  $\text{cm}^{-1}$  attributed to twist of the O–H. These stretches are provided by the presence of water adsorbed on the catalyst surface.<sup>25</sup> The band at 564  $\text{cm}^{-1}$  was assigned to the stretching bond of Cr–O.<sup>26</sup> The band related to Al–O was not well defined, due to the presence of various phases of alumina that caused an overlap of this band.

The TGA curve (Figure 1a) of carbonates obtained by co-precipitation shows a weight loss at 50-115 °C due to the adsorbed water. Another weight loss is observed between 110 °C and 400 °C and it is attributed to carbonate ion loss. TGA curve of catalyst (Figure 1b) does not show a significant loss or gain of mass, just the loss of adsorbed water in approximately 100 °C. TGA curve of CRAL confirms the absence of carbonate and residual nitrate, showing that the calcinations temperature and time used

were appropriate to eliminate waste products and form a solid with a high degree of purity.

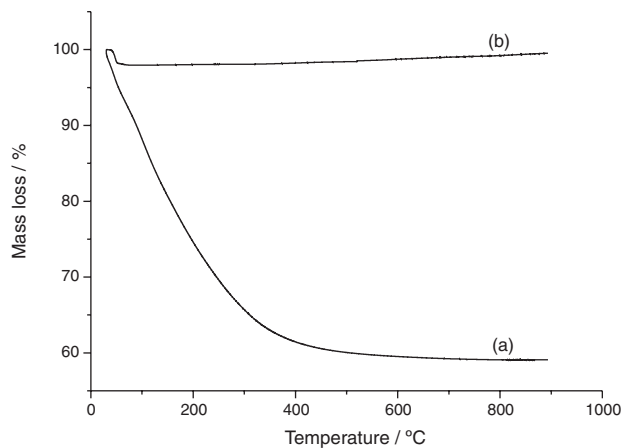


Figure 1. TG curves of (a) carbonates; (b) CRAL.

Elemental EDX-mapping (Table 1, Figure S2) has shown chromium highly dispersed and distributed homogeneously on all surface of alumina. The analysis has shown also that CRAL contains chromium, sodium, aluminum and oxygen in the ratio expected for  $(\text{Cr}_2\text{O}_3/\text{Na}_2\text{CrO}_4/\text{Al}_2\text{O}_3)$ , 0.25:0.25:0.50.

Table 1. EDX results

Element	Calculated / %	Found / %	Error / %
Cr	25.13	25.34	0.84
Al	26.46	25.87	2.23
O	41.30	42.08	1.89
Na	7.09	6.87	3.10

Figure 2 shows the XRD of CRAL where it can be seen a crystalline structure with some broad peaks due to the phases of alumina.  $2\theta = 37.46^\circ$  and  $67.23^\circ$  was attributed to  $\gamma$ -alumina,<sup>27</sup> and it was compared with JCPDS card No. 10-0425. The other crystalline phases of alumina, such as  $\theta$ - $\text{Al}_2\text{O}_3$  and  $\alpha$ - $\text{Al}_2\text{O}_3$ , are found when the temperature of calcination is above 900 °C.<sup>26</sup> Nonetheless, compounds calcined over this temperature do not represent an important pathway for the catalyst to the transesterification reaction. The best properties of the catalysts are found with calcination temperatures ranging from 400 °C to 600 °C.<sup>26</sup>

Xu *et al.*<sup>28</sup> described that as the Cr/Al ratio increases from 7% to 15%,  $\text{Cr}_2\text{O}_3$  diffraction peaks gradually appear, showing a crystalline solid. This fact indicated that the dispersion became poor with the increase of Cr content. The catalyst obtained in this study had 25% of  $\text{Cr}_2\text{O}_3$  and this explains the crystalline solid. The  $\text{Cr}_2\text{O}_3$  diffraction peaks were compared with JCPDS card No. 84-1616. The

$\text{Na}_2\text{CrO}_3$  evidenced by the presence of diffraction peaks in JCPDS No. 00-025-1107 with 25% may also explain the crystallinity of the solid.

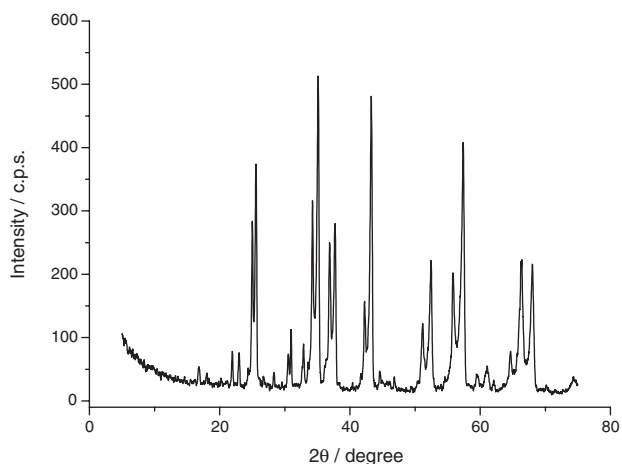


**Figure 2.** XRD of CRAL.

The SEM analysis (Figure 3) was carried out to investigate the morphology of CRAL, and it shows a particle size not defined. It can be observed different forms of particle size ranging from 1-3  $\mu\text{m}$ , or an agglomerate

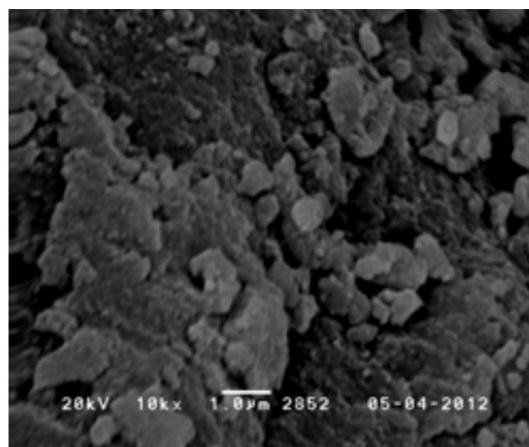
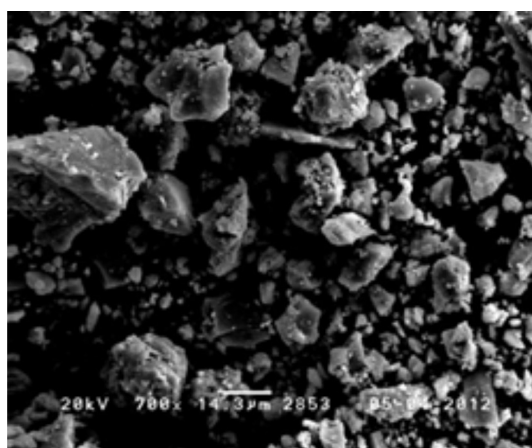


**Figure 3.** SEM of CRAL.

of particles. The particles show a typical particle size distribution of the alumina,<sup>29-31</sup> and sodium chromate that recovers the particles. This fact is in accordance to the phases found in XRD.

The pore size distributions of CRAL ranged from 2.9 to 7.0  $\mu\text{m}$ , being classified as mesoporous material.<sup>32</sup> The profile analysis of the CRAL isotherm (Figure 4) corroborates the classification given by the pore size distribution analysis, because the isotherm is of IV type, with hysteresis type III, being characteristic of mesoporous materials.<sup>33</sup>

The hysteresis at high pressures (0.4-1.0) are consistent with uniform and one-dimensional pores, however, the hysteresis of III type suggests an aggregate of particles with different pore geometries, as can be confirmed by SEM analysis. According to the BET method, the value found for the surface area of catalysis was 56  $\text{m}^2 \text{g}^{-1}$ .

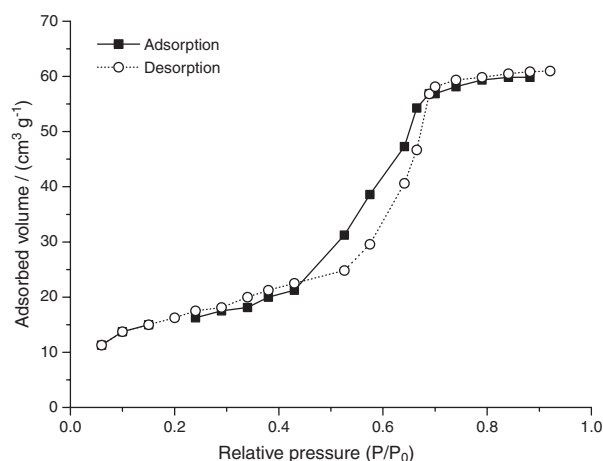


**Figure 4.** Nitrogen sorption isotherms of CRAL.

#### Acidity of catalyst

The determination of the type of sites in acids catalysts used for transesterification reactions is very important. One method for determining the Lewis and Brönsted acid sites is the impregnation of these sites with bases such as pyridine, 2,6-di-*tert*-butyl-pyridine, among others.<sup>33,34</sup> In this study, it was used the infrared absorption of pyridine (FTIR) as probe molecule to quantification of the Lewis and Brönsted acidity.<sup>35,36</sup> Thus, it was possible to differentiate between the Lewis (coordination of pyridine) and Brönsted (adsorption of pyridinium ion) acid sites and total acidity. The bands relating to the adsorption of pyridine in the Lewis (L) and Brönsted (B) acids sites are, respectively, 1435-1470 and 1515-1565  $\text{cm}^{-1}$ .<sup>37,38</sup> Figure S3 shows the IR spectra obtained to CRAL. In accordance with Gyftopoulou *et al.*<sup>39</sup> the acidic characteristic of mixed oxides is derived both from Brönsted (proton donor) and

Lewis (electron pair receiver) acid sites. The concentration of acid sites was calculated by equations 2 and 3. The results found were: Brönsted,  $160.39 \mu\text{mol g}^{-1}$  and Lewis,  $21.89 \mu\text{mol g}^{-1}$ . The total acidity was  $182.28 \mu\text{mol g}^{-1}$ . With increasing temperature, it is noted that the sites of Lewis decrease and the Brönsted increase. Brei *et al.*<sup>40</sup> have used FTIR spectra measurements to show that all Brönsted sites were transformed into Lewis acid sites at a calcination temperature of  $700^\circ\text{C}$  or above. Clearfield *et al.*<sup>41</sup> pointed that Brönsted acidity is believed to be present only for calcination below  $650^\circ\text{C}$ . Calcination temperature of CRAL catalyst was  $500^\circ\text{C}$ . Di Gregorio and Keller<sup>42</sup> have studied the tungstated zirconia (WZ), and claim that the required Lewis sites can turn into Brönsted sites by condensation. Similar results were seen for  $\text{WO}_3/\gamma\text{-Al}_2\text{O}_3$ .<sup>43</sup> Lopes *et al.*<sup>33</sup> have studied the effect of calcination temperature of tungstated zirconia catalyst in the transesterification and esterification reactions, and they found that the acidity of catalysts calcined at  $800^\circ\text{C}$  have predominance in Brönsted sites. Besides the fact of calcination temperature, Iglesias *et al.*<sup>44</sup> showed that the nature of the support ( $\text{ZrO}_2$ ,  $\text{Al}_2\text{O}_3$ ,  $\text{SiO}_2$  and  $\text{SnO}_2$ ) may influence the Lewis acidity. The XRD analyzes of CRAL show that the predominant phase of the  $\text{Al}_2\text{O}_3$  is  $\gamma$ -alumina. Soled *et al.*<sup>43</sup> found an increase in Brönsted acidity for  $\text{WO}_3$  on  $\gamma\text{-Al}_2\text{O}_3$  with increasing calcination temperature from  $500^\circ\text{C}$  to  $950^\circ\text{C}$ .

#### Characterization of methyl esters

Considering industrial and economic factors, it is important to evaluate the parameters that minimize the production costs of biodiesel, such as methanol/oil molar ratio and catalyst quantity.<sup>45</sup> Due to the dynamic equilibrium in the transesterification reaction, it is expected that the excess of alcohol increases the conversion rate. However, an excessive amount of alcohol should be avoided because it hinders the process of separation and purification, adversely affecting the properties of biodiesel. Generally, the catalysts used in reactions are expensive, so it is important to apply the minimum catalyst that provides the maximum conversion. GC technique was used to measure the conversion of babassu oil into methyl esters.

Stoichiometrically, the transesterification reaction requires three moles of methanol for each mole of triglyceride. Nonetheless, the excess of methanol is commonly employed in order to shift the reaction equilibrium towards the desired product side.<sup>46</sup> In general, the higher methanol/oil molar ratio is required for the acid-catalyzed process to obtain a higher reaction conversion,

in comparison with the base-catalyzed process.<sup>3</sup> The effect of methanol/oil molar ratio was investigated using 3% of solid catalyst, 15 h of reaction and  $70^\circ\text{C}$ . The results are shown in Figure 5a, and it can be seen that with increase in methanol/oil molar ratio, the conversion was gradually increased until reaching a maximum at 24:1 molar ratio; after that, the increase of molar ratio causes an intensive drop in FAME content. This fact could be explained for two reasons: (i) the hydrolysis of FAME happens during the reaction, resulting in reversible reaction; (ii) the fact that triglyceride molecules are chemisorbed on the active site of catalyst, where the carbonyl group forms a carbonium ion. If the methanol is in excess, the approaching to the carbocation enhances the rate conversion. The low conversion was used, in this work, due to the flooding of active sites with methanol molecules rather than triglyceride molecules.<sup>47</sup>

The effect of catalyst amount was also investigated using 15 h of reaction, 24:1 methanol/oil molar ratio at  $70^\circ\text{C}$ . When the catalyst quantity was increased from 1% to 3%, the conversion was gradually increased (Figure 5b). After 3% of loading, it was noted that the FAME conversion had a little decrease. With increasing loading, it is observed a small drop in FAME conversion, due to all the reactant molecules that have occupied the active sites of the catalyst, with excess of unoccupied active sites or with the great catalyst quantity and the reaction mixture becoming so much viscous, leading to the problem of mixing and separation, and decreasing the kinetic energy. Probably, the rate of reaction is controlled by the diffusion rate of reactants to the active site rather than the number of active sites.

The catalyst activity is influenced by various factors, such as catalytic area, pore volume, and the amount of sites available to realize the reaction. By textural data found for the CRAL catalyst, it was not observed a large surface area or a large pore volume; however, it proved to be very efficient for transesterification reaction. This fact can be explained by the high Brönsted acidity displayed by the catalyst. From these results, the optimum quantity of catalyst for this study was 3%, considering the mass of catalyst in relation to the mass of oil used in the transesterification reaction. TOF (turnover frequency) of FAME formation (at reaction time of 1.0 h), which represents the molecular number of FAME formed *per second per site* (basic or acid), has been calculated for CRAL catalyst and the result is  $24.5 \times 10^{-4} \text{ s}^{-1}$ . It can be seen that the values of TOF explain why the reaction has taken about 15 hours to achieve the maximum conversion, and the catalytic activity is related to both the amount and strength of acidic sites.<sup>48</sup>

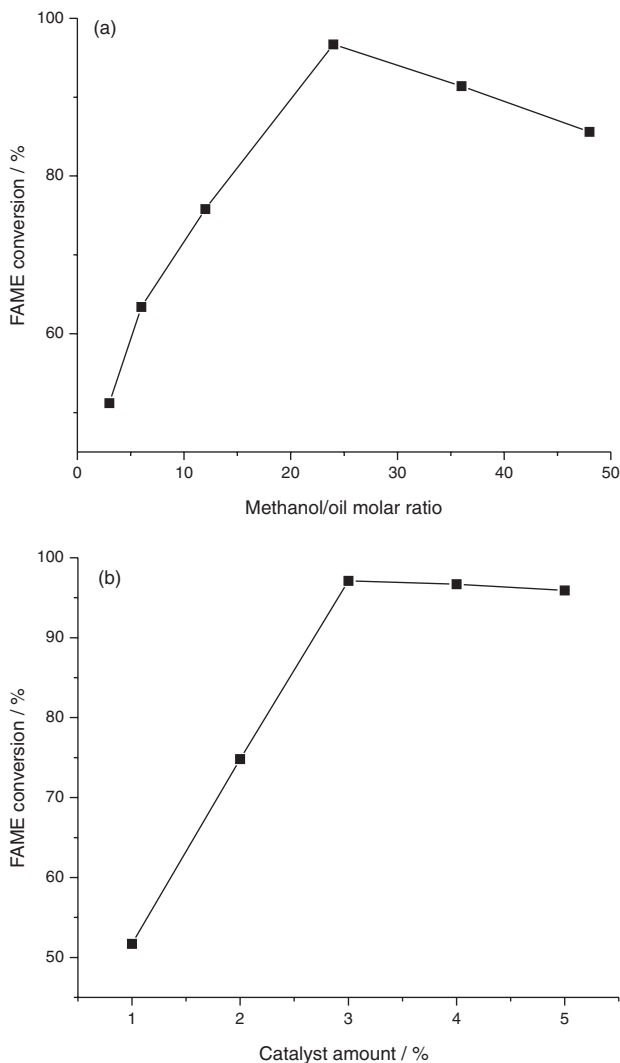


**Figure 5.** (a) Effect of molar ratio of babassu oil on conversion of FAMEs; (b) effect of catalyst amount on the conversion of FAMEs.

#### Effect of time on the conversion of FAMEs

Figure 6 shows the effect of time on the conversion of FAMEs at the catalysis of CRAL. The reaction time varied within the range of 0 h to 24 h. A gradual increase in the FAMEs conversion was observed with the increasing of time hour to hour until reaching 15 hours, when the FAMEs conversion reached 98.85%. After this time, the conversion was kept constant.

#### Kinetic of transesterification reaction

According to Kusdiana and Saka,<sup>49</sup> the thermal transesterification reaction is divided into three steps. Each step consumes 1 mol of methanol and forms 1 mol of ester.<sup>49</sup> By ignoring the intermediate reactions of diglyceride and monoglyceride, the three steps have been combined in a single step.<sup>50</sup> Upon optimization, it was found that the

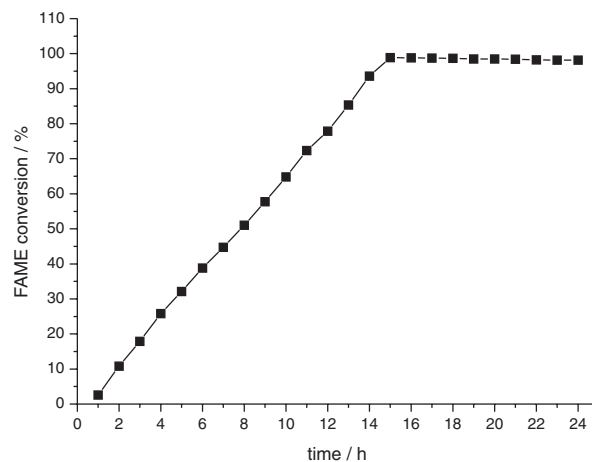


**Figure 6.** Effect of time on the conversion of FAMEs.

maximum conversion (98.6%) was obtained at the optimum conditions of catalyst amount of 3.0% relative to oil, methanol/oil molar ratio of 24:1 and 15 hours.

The transesterification reaction is reversible and, therefore, excess of alcohol is used to drive the reaction forward. Equation 5 shows the generalized transesterification reaction, where A is the triglyceride, B is alcohol, C is FAME's and D is glycerol.



In this reaction, 3 mole-equivalents of alcohol (B) react initially with a triglyceride (A) and, through three consecutive reverse (equilibrium) reactions, convert it in a stepwise manner to diglyceride, monoglyceride and, finally, to free glycerol; one mole-equivalent of the corresponding FAME's produced in every step of these reversible reactions. It is well known that if one of the reactants is taken in large excess, i.e., if the concentration of a given reactant is very high, then the rate of reaction depends on the concentration of the reactant which is taken in lower concentration. In case of transesterification reaction, the alcohol is used in large quantity. Some authors, as Vujicic *et al.*,<sup>51</sup> Sing and Fernando,<sup>52</sup> Ilgen,<sup>53</sup> Zang *et al.*,<sup>54</sup> Brahmkhatri and Patel,<sup>55</sup> described that the overall conversion of triglyceride into FAME's should follow a forth order reaction rate low, however due to a huge surplus of alcohol in the reaction mixture, the reaction could be safely considered as obeying the pseudo-first-order kinetic.

The data between  $\log C_A/C$  versus time in different temperatures (Figure 7) showed a good linear relationship, and support the hypothesis that the reaction is of pseudo-first order.<sup>56,57</sup>

The value of the reaction rate (k constant) was determined at different temperatures and the results

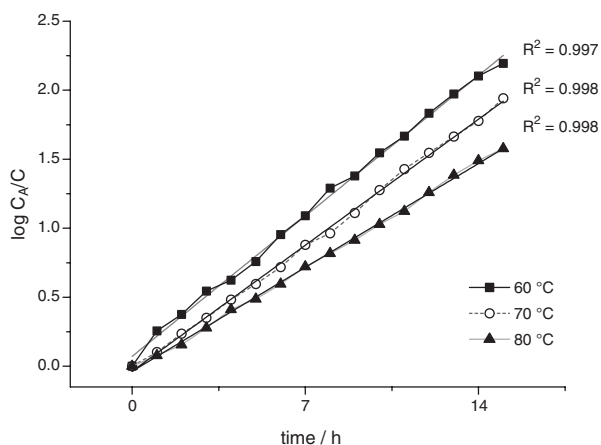


**Figure 7.** Fitting exponential of  $\log C_A/C$  versus time at different temperatures (methanol/oil molar ratio = 12:1, catalyst amount = 3.0 wt. % relative to oil).

were:  $k_{60} = 4.0373 \times 10^{-5} \text{ s}^{-1}$ ,  $k_{70} = 3.622 \times 10^{-5} \text{ s}^{-1}$  and  $k_{80} = 2.987 \times 10^{-5} \text{ s}^{-1}$ .

The apparent activation energy for the transesterification reaction could be calculated using the Arrhenius equation. It was plotted  $\ln k$  versus  $1/T$  graph (Figure 8), and the activation energy ( $E_a$ ) was calculated using the slope of curve, giving the result  $49.18 \text{ kJ mol}^{-1}$ ; pre-exponential factor was  $3.69 \times 10^{-5}$ . The activation energy found in the present work is compared with those reported in the literature by Brahmkhatri *et al.*<sup>55</sup> ( $44.6 \text{ kJ mol}^{-1}$ ), Aranda *et al.*<sup>58</sup> ( $42 \text{ kJ mol}^{-1}$ ), Sarkara *et al.*<sup>59</sup> ( $39.5 \text{ kJ mol}^{-1}$ ) and Patel *et al.* ( $52.4 \text{ kJ mol}^{-1}$ ).<sup>60</sup>

If the reaction rate is diffusion limited/mass transfer or it is truly governed by the chemical step, the catalyst is

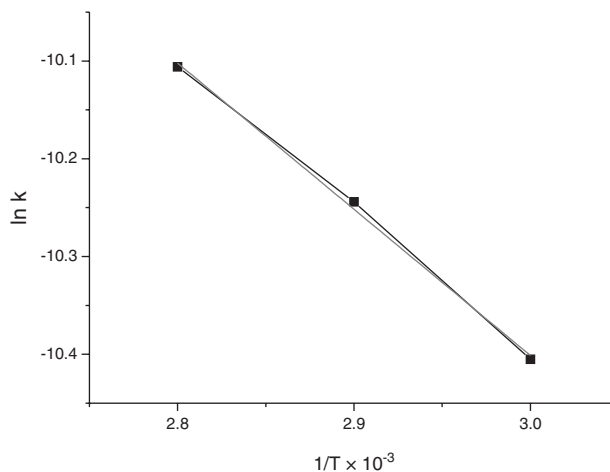
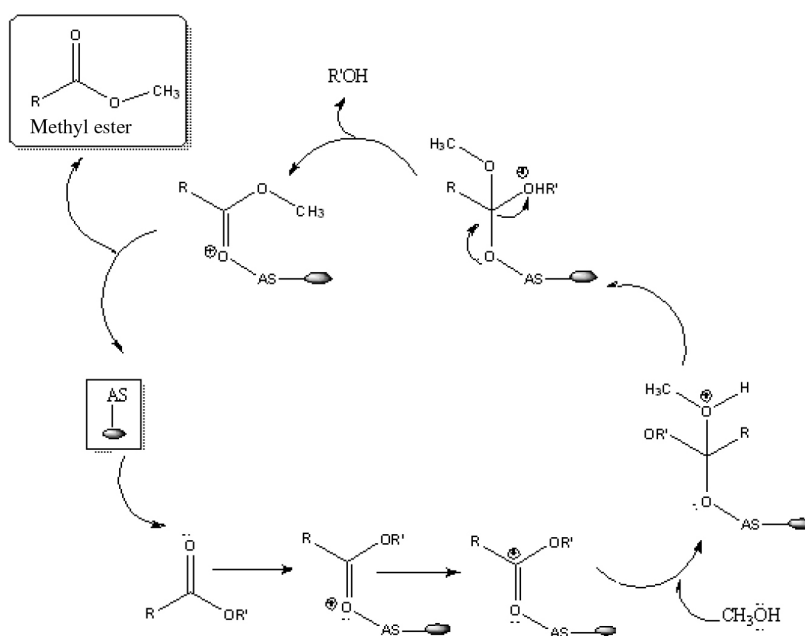


**Figure 8.** Arrhenius plot for determination of activation energy.

being used to its maximum capacity. It is reported that the activation energy for diffusion limited reactions is as low as  $10\text{--}15 \text{ kJ mol}^{-1}$ , and for reactions whose rate is governed by a truly chemical step, it usually shows activation energy excess of  $25 \text{ kJ mol}^{-1}$ .<sup>44</sup> In this case, it was possible to affirm that the rate is truly governed by chemical step.

In accordance with Brahmkhatri *et al.*<sup>61</sup> and Sani *et al.*<sup>62</sup> the mechanism of transesterification using Brönsted acid is shown in Scheme 1. At first, occurs an interaction between Brönsted acid sites and carbonyl oxygen of triglycerides to form carbocation. The nucleophilic attack of alcohol to the carbocation produces a tetrahedral intermediate, and then occurs  $R'OH$  elimination (Scheme 1) to form the alkyl ester of triglyceride. If compared the activity of basic catalyst



**Scheme 1.** Solid acid catalyzed transesterification, AS = acid site on the catalyst surface, R = alkyl group of fatty acid, R' = alkyl group of triglyceride.

with acid catalyst, clearly the acid catalyst acts more slowly in transesterification reactions. Thus, a greater amount of catalyst than for basic catalyst is required.<sup>63</sup>

#### Leaching, heterogeneity and reusability test

The reusability and stability of catalyst were tested using a methanol to oil molar ratio of 24:1 and catalyst to oil mass ratio of 3.0%, reaction time of 15 h; these conditions resulted in the best conversion in this work. This test is an important characteristic to evaluate its economical application. Table 2 shows the results obtained for the catalyst activity during the reusability and leaching tests. In accordance with Olutoye *et al.*<sup>64</sup> there are some reasons for the catalytic activity loss; (i) the original sites can be blocked by large molecule inhibiting the diffusion of oil molecules, intermediate or product species into the pores; (ii) loss of active component during the washing and recovery of catalyst for the subsequent runs; (iii) leaching of active component of the catalyst with the increase of reaction cycle. The results indicated that CRAL is active to biodiesel production for one cycle. After that, the conversion had a considerable drop, indicating a leaching of about 13% of the principal species of catalyst, demonstrating that the catalyst is not totally heterogeneous and it loses its activity after the first run. The atomic absorption spectrometry (AAS) technique was used to

evaluate the chromium degree of leaching into biodiesel and the results are shown in Table 2. Probably, the reason that the catalyst was leaching is due to the support used, in this case,  $Al_2O_3$ . This problem could be solved by changing the support and using for example, magnetic tape.

**Table 2.** Conversion of triglycerides over reused catalyst and heterogeneity test

	FAME <sup>a</sup> oil + methanol / %	Reusability FAME <sup>a</sup> / %	Cr / ppm
Blank test	38	–	–
1 <sup>st</sup> run	–	98.85	57.77
2 <sup>nd</sup> run	–	37.536	55.13
3 <sup>rd</sup> run	–	25.68	54.91
4 <sup>th</sup> run	–	15.46	54.86

<sup>a</sup>FAME: fatty acid methyl ester.

Before using fuel in machines, it is necessary to ensure its quality. For that, there are standards and specifications established by the supervisory agencies, whether national or international. In Brazil, the agency that sets the rules for specifying and marketing of biodiesel is the National Agency of Petroleum, Natural Gas and Biofuels (ANP).

Table 3 presents the values of the physicochemical properties of biodiesel and the values are within ANP specification by the 14/2012 resolution.

**Table 3.** Physical-chemical properties of biodiesel

Parameter	Biodiesel	ANP <sup>a</sup> 14/2012	Standard	
			ASTM D	EN/ISSO
Cinematic viscosity 40 °C / (mm <sup>2</sup> s <sup>-1</sup> )	3.2	3.0-6.0	445	–
Density / (g cm <sup>-3</sup> )	0.87	0.85-0.90	4052	–
Maximum water content / ppm	250	500	6304	–
Maximum acidity index / (mg KOH g <sup>-1</sup> )	0.4	0.5	–	14104
Maximum iodine index / (g 100 g <sup>-1</sup> )	22.5	120	–	14111
Maximum methanol / (wt.%)	0.00	0.20	–	14110
Maximum sulfur content / (wt.%)	0.04	0.50	4229	–
Maximum copper corrosivity	1 <sup>st</sup>	1 <sup>st</sup>	130	–
Maximum CFPP <sup>b</sup> / °C	–5.0	19.0	6371	–
Minimum flash point / °C	111	100	–	3679
Free glycerin / (wt.%)	0.00	0.02	–	14105
Total glycerin / (wt.%)	0.10	0.38	–	14105
Monoglyceride / %	0.37	1.00	–	14105
Diglyceride / %	0.05	0.25	–	14105
Triglyceride / %	0.00	0.25	–	14105
Esther content / (wt.%)	97.51	96.5	–	–

<sup>a</sup>Agency of Petroleum, Natural Gas and Biofuels (ANP); <sup>b</sup>CFPP: cold filter plugging point.

## Conclusions

The acid catalyst (CRAL) was prepared and the analyses of DRX, EDX and SEM show that the catalyst is a mixture of  $\text{Cr}_2\text{O}_3/\text{Na}_2\text{CrO}_4/\text{Al}_2\text{O}_3$  in the following proportion (0.25:0.25:0.50), respectively. The total acidity was  $182.28 \mu\text{mol g}^{-1}$ , but the major acidity was in Brönsted sites. The TOF found in this study was  $24.4 \times 10^{-4} \text{ s}^{-1}$ . The textural analyses of catalyst show that the surface area is  $56 \text{ m}^2 \text{ g}^{-1}$ , and the pore size distribution and hysteresis profile classifies it as mesoporous material. The catalyst has catalyzed the transesterification reaction of babassu oil even containing 5% of FFA. The conversion obtained to transesterification of babassu oil was 98.6%, after 15 h of reaction. The methanol/oil molar ratio of 24:1 and 3 wt.% of catalyst loading were employed. The kinetic study shows that the transesterification reaction follows first order rate law and the activation energy was  $49.18 \text{ kJ mol}^{-1}$ , being the rate truly governed by chemical step. Also the activity of the catalyst is comparable to the traditional sulfuric acid catalyst. The test of reusability shows that the catalyst works for one cycle, since a considerable drop occurred, indicating a leaching of about 13% of chromium species. This fact demonstrated that the catalyst obtained in this work is not totally heterogeneous. The biodiesel produced in this study follows the 14/2012 Resolution of ANP specification.

## Supplementary Information

Supplementary data are available free of charge at <http://jbcs.sbq.org.br> as PDF file.

## Acknowledgements

We would like to thank the agencies funding CAPES (PROCAD), FAPEPI, CNPq, FINEPI, and the following laboratories, LIEC of São Carlos, CEMPEQC Araraquara-SP and LAPETRO-UFPI, where the characterizations of the catalysts and methyl esters were made.

## References

- Prado, A. G. S.; *Quim. Nova* **2003**, *26*, 738.
- Liu, Y. O.; Loreto, E.; Goodwin Jr., J. G.; Mo, X.; *Appl. Catal., A* **2007**, *331*, 138.
- Xie, W.; Wang, H.; Li, H.; *Ind. Eng. Chem. Res.* **2012**, *51*, 225.
- Helwani, Z.; Othaman, M. R.; Aziz, N.; Kim, J.; Fernando, W. J. N.; *Appl. Catal., A* **2009**, *363*, 1.
- Zheng, S.; Kates, M.; Dube, M. A.; McLean, D. D.; *Biomass Bioenergy* **2006**, *30*, 267.
- di Serio, M.; Tesser, R.; Dimiccoli, M.; Cammarota, F.; Nastasi, M.; Santacesaria, E.; *J. Mol. Catal. A: Chem.* **2005**, *239*, 111.
- Lotero, E.; Liu, Y. J.; Lopez, D. E.; Suwannakarn, K.; Bruce, D. A.; Goodwin Jr, J. G.; *Ind. Eng. Chem. Res.* **2005**, *44*, 5353.
- Goff, M. J.; Bauer, N. S.; Lopes, S.; Sutterlin, W. R.; Suppes, G. J.; *J. Am. Oil Chem. Soc.* **2004**, *81*, 415.
- Kulkarni, M. G.; Gopinath, R.; Meher, L. C.; Dali, A. K.; *Green Chem.* **2006**, *8*, 1056.
- Sani, Y. M.; Daud, W. M. A. W.; Aziz, A. R. A.; *Appl. Catal., A* **2014**, *470*, 140.
- Sharma, Y. C.; Singh, B.; Korstad, J.; *Fuel* **2011**, *90*, 1309.
- Jitputti, J.; Kitiyanan, B.; Rangsunvigit, P.; Bunyakiat, K.; Attanatho, L.; Jenvanitpanjakul, P.; *Chem. Eng. J.* **2006**, *116*, 61.
- Lopez, D. E.; Suwannakarn, K.; Bruce, D. A.; Goodwin Jr, J. G.; *J. Catal.* **2007**, *247*, 43.
- Delfort, B.; Hillion, G.; le Penec, D.; Lendresse, C.; *US pat. US2005261509 A*, **2005**.
- Li, H.; Xie, W.; *J. Am. Oil Chem. Soc.* **2008**, *85*, 655.
- Xie, W.; Yang, D.; *Bioresour. Technol.* **2011**, *102*, 9818.
- Li, H.; Xie, W.; *Catal. Lett.* **2006**, *107*, 25.
- Bae, J. W.; Kim, S. M.; Kang, S. H.; Chary, K. V. R.; Lee, Y. J.; Kim, H. J.; Jun, K. W.; *J. Mol. Catal. A: Chem.* **2009**, *311*, 7.
- Xie, W.; Yang, D.; *Bioresour. Technol.* **2012**, *119*, 60.
- Huang, P.; Jiang, H.; Zhang, M.; *J. Rare Earths* **2012**, *30*, 524.
- Wang, Z.; Li, X.; Zhang, Y.; Shi, L.; Sun, Q.; *Chin. J. Catal.* **2012**, *33*, 1139.
- Ivanova, A. S.; *Kinet. Catal.* **2012**, *53*, 425.
- Emeis, C. A.; *J. Catal.* **1993**, *141*, 347.
- Emin, S. U.; Erol, S.; *Bioresour. Technol.* **2012**, *106*, 178.
- Nakamoto, K.; *Infrared and Raman Spectra of Inorganic and Coordination Compounds, Part A*; John Wiley: New York, 1997.
- Caland, L. B.; Santos, L. S. S.; Moura, C. V. R.; Moura, E. M.; *Catal. Lett.* **2009**, *128*, 392.
- Xuea, Y.; Lina, J.; Fana, Y.; Li, J.; Elsanousi, A.; Xua, X.; Liuc, D.; Huang, Y.; Hua, L.; Liua, Y.; Menga, F.; Zoub, J.; Tanga, C.; *J. Cryst. Growth* **2013**, *382*, 52.
- Xu, L.; Wang, Z.; Song, H.; Chou, L.; *Catal. Commun.* **2013**, *35*, 76.
- Gao, Y.; Huang, Z.; Fang, M.; Liu, Y. G.; Haung, S.; Ouyang, X.; *Powder Technol.* **2012**, *226*, 269.
- Bay, Y.; Xu, H.; Zhang, Y.; Li, Z.; *J. Wuhan Univ. Technol., Mater. Sci. Ed.* **2008**, *23*, 181.
- Mehta, S.; Simmons, G. W.; Klier, K.; Herman, R. G.; *J. Catal.* **1979**, *57*, 339.
- Sing, K. S. W.; Everett, D. H.; Haul, R. A. W.; Moscou, L.; Pierotti, R. A.; Rouquerol, J.; Siemieniewska, T.; *Pure Appl. Chem.* **1985**, *57*, 603.
- López, D. E.; Suwannakarn, K.; Bruce, D. A.; Goodwin Jr, J. G.; *J. Catal.* **2007**, *247*, 381.

34. Brown, H. C.; Johanneson, R. B.; *J. Am. Chem. Soc.* **1953**, *75*, 16.
35. Busca, G.; *Catal. Today* **1998**, *41*, 191.
36. Chmielarz, L.; Kustrowski, P.; Drozdek, M.; Dziembaj, R.; Cool, P.; Vansant, E. F.; *Catal. Today* **2006**, *114*, 319.
37. Yazıcı, D. T.; Bilgic, C.; *Surf. Interface Anal.* **2010**, *42*, 959.
38. Layman, K. A.; Ivey, M. M.; Hemminger, J. C.; *J. Phys. Chem. B* **2003**, *107*, 8538.
39. Gyftopoulou, M. E.; Millan, M.; Bridgwater, A. V.; Dugwell, D.; Kandiyoti, R.; Hriljac, J. A.; *Appl. Catal., A* **2005**, *282*, 205.
40. Brei, V. V.; Melezhyk, O. V.; Prudius, S. V.; Tel'biz, G. M.; Oranska, O. I.; *Adsorpt. Sci. Technol.* **2005**, *23*, 109.
41. Clearfield, A.; Serrete, G. P. D.; Khazisyed, A.; *Catal. Today* **1994**, *20*, 295.
42. di Gregorio, F.; Keller, V.; *J. Catal.* **2004**, *225*, 45.
43. Soled, S. L.; McVicker, G. B.; Murrel, L. L.; Sherman, L. G.; Dispenziere, N. C.; Hsu, S. L.; Waldman, D.; *J. Catal.* **1988**, *111*, 286.
44. Macht, J.; Baertsch, C. D.; May-Lozano, M.; Soled, S. L.; Wang, Y.; Iglesia, E.; *J. Catal.* **2004**, *227*, 479.
45. Freedman, B.; Pryde, E. H.; Mounts, T. L.; *J. Am. Oil Chem. Soc.* **1984**, *61*, 1638.
46. Li, Y.; Qiu, F.; Yang, D.; Li, X.; Sun, P.; *Biomass Bioenergy* **2011**, *35*, 2787.
47. Aghabarari, B.; Dorostkar, N.; Martinez-Huerta, M. V.; *Fuel Process. Technol.* **2014**, *118*, 296.
48. Xia, S.; Guo, X.; Mao, D.; Shi, Z.; Wu, G.; Lu, G.; *RSC Adv.* **2014**, *4*, 51688.
49. Kusdiana, D.; Saka, S.; *Fuel* **2011**, *80*, 693.
50. Vujicic, D.; Comic, D.; Zarubica, A.; Micic, R.; Boskovi, G.; *Fuel* **2010**, *89*, 2054.
51. Singh, A. K.; Fernando, S. D.; *Chem. Eng. Technol.* **2007**, *30*, 1716.
52. Ilgen, O.; *Fuel Process. Technol.* **2012**, *95*, 62.
53. Zhang, L.; Sheng, B.; Xin, Z.; Liu, Q.; Sun, S.; *Bioresour. Technol.* **2010**, *101*, 8144.
54. Brahmkhatri, V.; Patel, A.; *Appl. Catal., A* **2011**, *403*, 161.
55. Birla, A.; Singh, B.; Upadhyay, S. N.; Sharma, Y. C.; *Bioresour. Technol.* **2012**, *106*, 95.
56. Aranda, D. A. G.; Santos, R. T. P.; Neyda, C. O.; Tapanes, A. L. D.; Ramos, O. A. C.; *Catal. Lett.* **2008**, *122*, 20.
57. Sarkara, A.; Ghosh, S. K.; Pramanika, P.; *J. Mol. Catal. A: Chem.* **2010**, *327*, 73.
58. Granados, M. L.; Alonso, D. M.; Alba-Rubio, A. C.; Mariscal, R.; Ojeda, M.; Brettes, P.; *Energy Fuels* **2009**, *23*, 2259.
59. Carvalho, L. M. G.; Abreu, W. C.; Silva, M. G. O.; Lima, J. R. O.; Oliveira, J. E.; Matos, J. M. E.; Moura, C. V. R.; Moura, E. M.; *J. Braz. Chem. Soc.* **2013**, *24*, 550.
60. Patel, A.; Brahmkhatri, V.; *Fuel Process. Technol.* **2013**, *113*, 141.
61. Brahmkhatri, V.; Patel, A.; *Appl. Catal., A* **2011**, *403*, 161.
62. Sani, Y. M.; Daud, W. M. A. W.; Aziz, A. R. A.; *Appl. Catal., A* **2014**, *470*, 140.
63. Nakayama, M.; Tsuto, K.; Hirano, T.; Sakai, T.; Kawashima, A.; Kitagawa, H.; *US pat. 6,960,672 B2* **2005**.
64. Olutoye, M. A.; Wong, C. P.; Chin, L. H.; Hameed, B. H.; *Fuel Process. Technol.* **2014**, *124*, 54.

Submitted: July 9, 2015

Published online: October 27, 2015

FAPESP has sponsored the publication of this article.